Iranian Journal of Science and Technology, Transactions of Mechanical Engineering (2021) 45:879–889
https://doi.org/10.1007/s40997-020-00356-7

RESEARCH PAPER

Nonlinear Vibration and Tip Tracking of Cantilever Flexoelectric Nanoactuators

Hossein Vaghefpour[1]

Received: 31 December 2019 / Accepted: 20 February 2020 / Published online: 7 March 2020
© Shiraz University 2020

Abstract

This paper examines the nonlinear vibration and tracking of cantilever nanoactuators made of isotropic nanodielectric materials with flexoelectric effect. The nonlinear governing equation of Euler–Bernoulli nanoactuators is derived based on non-classical continuum mechanics making use of material length scale parameters. By employing a higher-order curvature relation, the governing nonlinear partial deferential equations of motion are obtained by using the Hamilton's principle. Incorporating the Galerkin method, the nonlinear partial deferential equation is reducing into a set of nonlinear ordinary differential equations. The obtained reduced-order model is solved by a perturbation method for free vibration response in semi-closed form. By introducing a new set of variables, the state space model of nanobeam is derived. The sliding mode control algorithm is employed to achieve a desired output for tip tracking, and Lyapunov stability theory is used to prove convergence in finite time. The effectiveness of the proposed control algorithm and input voltage is illustrated by numerical simulations. Regarding to the finding of this paper, it can be found that the sliding mode controller has better performance than linear controller, e.g., fuzzy controller.

Keywords Size-dependent piezoelectricity · Nanobeam · Nonlinear tracking · Perturbation method · Flexoelectricity · Nonlinear vibration.

1 Introduction

Micro- and nanosize mechanical systems are widely used in modern devices. As well known, in the classical continuum theory, only macroscopic effects are taken into consideration; however, some experimental and theoretical studies show that length scale parameters play a major role on the mechanical behavior of micro-/nanostructures (Akgoz and Civalek 2012). The existing size-dependent theories, which include at least one additional or internal material length scale parameter (Akgoz and Civalek 2017), were used in several works to derive the governing equations of nanostructures, including the modified couple stress theory (Krysko et al. 2019; Akgoz and Civalek 2013), the strain gradient theory (Arefia et al. 2018; Akgoz and Civalek 2012), Eringen's the nonlocal theory (Ebrahimi and Barati 2017b; Ebrahimi et al. 2019; Numanoglu et al. 2018) and the surface elasticity model (Ansari et al. 2013). With the novel manufacturing methods for fabricating small-scale structures, the applications of nanostructures have extended rapidly (Yekrangisendi et al. 2019). Typical cantilever flexoelectric nanobeams thanks to the electromechanical coupling effects are the subject of intensive studies in the field of nano-/microelectromechanical systems (N/MEMS). They have been extensively used as sensors and actuators (Cao et al. 2015). Piezoelectric and flexoelectric materials are also employed for vibration control (Koszewnika 2018), noise control systems (Casadei et al. 2010), data collection (Sumali et al. 2001), actuators (Liu et al. 2015), telecommunication and sensor networks (Hao and Liao 2010), energy harvesting (Managheb et al. 2018; Rojas et al. 2019) and shape control of structures (Donthireddy and Chandrashekhara 1996). However, size-dependent linear electromechanical coupling has been reported in isotropic dielectrics (Mishima et al. 1997; Cross 2006; Baskaran et al. 2011) and the classical piezoelectric theory describes the relation between electric polarization and uniform strain in non-centrosymmetric dielectrics at macroscales. In small scale, when the strain gradient is considered in solids, linear

✉ Hossein Vaghefpour
h.vaghefpour@iauabadan.ac.ir

[1] Department of Mechanical Engineering, Abadan Branch, Islamic Azad University, Abadan, Iran

electromechanical coupling arises. This size-dependent electromechanical effect is known as the flexoelectric effect (Maranganti et al. 2006). On the other word, in micro- and nanoscale, the dielectric polarization depends not only on the strain tensor, but also on the curvature tensor. Thus, size-dependent (micro/nano) structures must be analyzed properly in different mechanical aspects and this process cannot be performed using classical continuum theory (Ebrahimia and Barati 2017a). Therefore, it is necessary to employ a size-dependent piezoelectricity, which accounts for the micro- and nanostructures. The first step toward developing size-dependent electromechanical theories is the establishment of the size-dependent continuum mechanics theory (Hadjesfandiari and Dargush 2011). It should be pointed out that many size-dependent theories based on the modified couple stress (Krysko et al. 2019), the strain gradient theory (Arani et al. 2015; Arefia et al. 2018), the nonlocal theory (Ke et al. 2012; Ebrahimi and Barati 2017b) and the surface elasticity model (Ansari et al. 2013) were used in several works to derive the governing equations of piezoelectric nanobeams. For this purpose, some researchers have illustrated the size effect in flexoelectric properties and linear electromechanical coupling in all classes of dielectric materials even for centrosymmetric crystals (Ebnali Samani and Tadi Beni 2018; Baskaran et al. 2011; Rojas et al. 2019). Many studies investigated the mechanical and electrical equations of the micro- and nanostructures by considering flexoelectricity effect (Nateghi et al. 2012). A size-dependent piezoelectricity theory, based on the electromechanical formulation, was developed by Hadjesfandiari (2013). The flexoelectricity theory developed by Hadjesfandiari (2013) introduces a compatible theory for piezoelectric and dielectric materials at the micro- and nanoscale. Most of micro-/nanosystems operate based on vibration of mechanical elements such as micro-/nanobeams, plates and wires; so study of vibration and control of micro-/nanomechanical elements is of great importance (Esmaeili and Beni 2019). On the other hand, mechanical vibrating elements are used in a large number of NEMS, for sensing and actuating. In these systems, it is important to achieve high sensitivity by accurate model. In this field, the most works use the von-Karman strain–displacement relationship for the nonlinear analysis, which leads to the linear equations of motion for the clamped-free beams (Vaghefpour et al. 2018). In this regard, many researchers have been studying vibration and control of micro-/nanostructures. Alsaleem and Younis (2011) by using delay feedback controllers stabilize MEMS resonators especially near pull-in point. Wang (1998) investigated the feedback control of vibrations in cantilever beams with electrostatic actuators. The effects of the control gains on an electrically actuated resonator were examined by Shao et al. (2013). The control of chaotic motion of a MEMS resonator was examined by Siewe (2011), to indicate that reducing the amplitude of the parametric excitation can control the chaotic motion of a MEMS resonator. Seleim et al. (2012) considered a closed-loop control for a MEMS resonator and obtained optimal operating regions for the resonator. Vatankhah et al. (2013) brought up the problem of boundary stabilization by considering linear boundary control law to stabilize vibrating a non-classical microbeam. Quoc and Slava (2015) developed a nonlinear control algorithm to control force vibration of a microelectromechanical.

It can be seen from the literature review, although several studies have developed the dynamic modeling and vibration analysis of non-classical micro-/nanobeams in the recent years, nonlinear tracking control of the flexoelectric nanobeams has not been considered yet. The contributions of this paper are to derive the nonlinear model of the flexoelectric cantilever nanobeam as an actuator on the basis of the size-dependent piezoelectric theory implementing a higher-order curvature relation. The equation of motion for the inextensible cantilever flexoelectric nanobeams is obtained taking into account the geometric nonlinearities while neglecting shear deformation and rotary inertia. For order reduction in the beam equation of motion into ODEs, the Galerkin method is employed. The perturbation method is applied on the obtained ODEs to determine the vibration responses (Sect. 2). Nonlinear tip tracking control algorithms for flexoelectric cantilever nanobeam are developed based on sliding mode, and the simulation results are presented (Sect. 3). The results demonstrate the effectiveness of the presented algorithms. The main obtained outcomes are discussed in Sect. 4.

2 Nonlinear Modeling

The schematic isotropic flexoelectric cantilever nanoactuator with length L, width b and thickness h considered in this work is depicted in Fig. 1. Employing the size-dependent piezoelectricity theory (Hadjesfandiari 2013), the non-dimensional equations of motion and the related boundary conditions of the cantilever flexoelectric nanoactuators can be expressed, respectively, as Vaghefpour (2019):

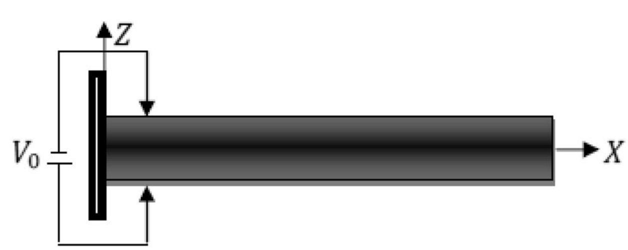

Fig. 1 Schematic view of a flexoelectric nanoactuator

$$L_S w_{,xxxx} + G w_{,x}^2 w_{,xxxx} + 4G w_{,x} w_{,xx} w_{,xxx} + G w_{,xx}^3 + I_0 w_{,\tau\tau} = 0 \tag{1}$$

and

$$\delta w|_0 = 0 \quad \text{and} \quad L_S w_{,xxx} + G w_{,x}^2 w_{,xxx} + G w_{,x} w_{,xx}^2 \Big|^1 = 0$$
$$\delta(w_{,x})|_0 = 0 \quad \text{and} \quad \left[L_S w_{,xx} + G w_{,x}^2 w_{,xx} - F V_0(t) \right] \Big|^1 = 0 \tag{2}$$

where

$$L_S = (EI + A_{11})\frac{L^2}{h^2}, \quad G = (\lambda + 2\mu)I, \quad I_0 = \frac{(\lambda + 2\mu)IL^2}{h^2}, \quad \text{and} \quad F = \frac{2bL^4 f}{h^3} \tag{3}$$

A reduced-order model is obtained by discretization of the PDE, i.e., Eq. (1), with the corresponding boundary conditions, i.e., Eq. (2). One can approximate the displacement of the flexoelectric nanoactuator as Rafiepour et al. (2013):

$$w(x,t) = \sum_{i=1}^{n} q_i(t)\phi_i(x) \tag{4}$$

The reduced order of the equation of motion (EOM) of nanoactuator will be derived through the Galerkin method leading to:

$$\mathbf{M}\ddot{\mathbf{q}}(t) + \mathbf{K}\mathbf{q}(t) + \mathbf{B}\mathbf{q}^3(t) = \mathbf{E}V_0(t) \tag{5}$$

where $\mathbf{q}(t) = [q_i(t)]^{\mathsf{T}}$; **M**, **K** and **B** are the time-dependent vector of generalized coordinates, the mass matrix, the linear stiffness matrix and the nonlinear stiffness matrix, respectively; and T stands for the transpose. The elements of **M**, **K** and **B** matrices and **C** vector are given, respectively, by:

$$M_{ij} = I_0 \int_0^1 \phi_i \phi_j \mathrm{d}x, \quad K_{ij} = L_S \int_0^1 \phi_i'' \phi_j'' \mathrm{d}x, \quad B_{ij} = G \int_0^1 (\phi_i'' \phi_i'^2 \phi_j'' + \phi_i''^2 \phi_i' \phi_j')\mathrm{d}x, \quad E_j = F\phi_j'(1) \tag{6}$$

where $\phi' = \frac{\mathrm{d}\phi}{\mathrm{d}x}$.

2.1 Nonlinear Vibration Analysis

The parameterized perturbation method (PPM) is employed to develop the nonlinear vibration response of equations of motion, i.e., Eq. (5). At first, Eq. (5) is reshuffled as follows:

$$\ddot{q}(t) + \Omega q(t) + \gamma q^3(t) = \Gamma \tag{7}$$

where $\Omega = M^{-1}K$, $\gamma = M^{-1}B$, and $\Gamma = M^{-1}HV_0$.

By introducing a new set of variables $q = pS$, $S = S_0 + p^2 S_1$, and $\Omega = \omega_0^2 + p^2\omega_1$ (Barari et al. (2011)) and substituting the defined variables into Eq. (7), one can obtain:

$$p(\ddot{S}_0 + p^2\ddot{S}_1) + (\omega_0^2 + p^2\omega_1)p(S_0 + p^2 S_1) + \gamma p^3 (S_0 + p^2 S_1)^3 = \Gamma \tag{8}$$

Equating the coefficients of the same order of p yields the following ordered equations:

$O(p^1)$:

$$\ddot{S}_0 + \omega_0^2 S_0 = \frac{\Gamma}{p}, \qquad S_0(0) = \dot{S}_0(0) = 0 \tag{9}$$

$O(p^3)$:

$$\ddot{S}_1 + \omega_0^2 S_1 + \omega_1 S_0 + \gamma S_0^3 = 0, \qquad S_1(0) = \dot{S}_1(0) = 0 \tag{10}$$

The first-order equation, i.e., Eq. (9), delivers the first-order solution as:

$$S_0 = \frac{\Gamma}{p\omega_0^2}(1 - \cos\omega_0 t) \tag{11}$$

Substituting the first-order solution, i.e., Eq. (11) into Eq. (10), yields:

$$\ddot{S}_1 + \omega_0^2 S_1 + \omega_1 \frac{\Gamma}{p\omega_0^2}(1 - \cos\omega_0 t) + \gamma \left(\frac{\Gamma}{p\omega_0^2}(1 - \cos\omega_0 t) \right)^3 = 0 \tag{12}$$

Reshuffling Eq. (12) results in:

$$\ddot{S}_1 + \omega_0^2 S_1 + \omega_1 \frac{\Gamma}{p\omega_0^2} + \frac{5}{2}\gamma \left(\frac{\Gamma}{p\omega_0^2} \right)^3 - \left(\omega_1 \frac{\Gamma}{p\omega_0^2} + \frac{15}{4}\gamma \left(\frac{\Gamma}{p\omega_0^2} \right)^3 \right)\cos\omega_0 t + \frac{3}{2}\gamma \left(\frac{\Gamma}{p\omega_0^2} \right)^3 \cos\omega_0 2t - \frac{1}{4}\gamma \left(\frac{\Gamma}{p\omega_0^2} \right)^3 \cos\omega_0 3t = 0 \tag{13}$$

Following the common procedure of perturbation methods (see, for example, Alsaleem and Younis 2011) and avoiding the presence of the secular term $(\omega_1 \frac{\Gamma}{p\omega_0^2} + \frac{15}{4}\gamma(\frac{\Gamma}{p\omega_0^2})^3) = 0$:

$$\omega_1 = -\frac{15}{4}\gamma \left(\frac{\Gamma}{p\omega_0^2} \right)^2 \tag{14}$$

Subsequently, one can obtain $\omega_0^2 = \Omega + \frac{15}{4}\gamma(\frac{\Gamma}{\omega_0^2})^2$.

After elimination of the secular term from Eq. (12), the corresponding solution reads as:

$$S_1 = \frac{\gamma \Gamma^3}{p^3 \omega_0^8}\Big(-\frac{95}{32}\cos\omega_0 t + \frac{1}{2}\cos 2\omega_0 t - \frac{1}{32}\cos 3\omega_0 t + \frac{10}{4}\Big) \tag{15}$$

Substituting the first- and third-order solutions, respectively, Eqs. (11) and (15) into expanded form of S, i.e., $S = S_0 + p^2 S_1$, and considering $q = pS$, the nonlinear solution of Eq. (7) can be expressed as:

$$q = \frac{\Gamma}{\omega_0^2}\big(1 - \cos\omega_0 t\big) + \frac{\gamma \Gamma^3}{\omega_0^8}\Big(-\frac{95}{32}\cos\omega_0 t + \frac{1}{2}\cos 2\omega_0 t - \frac{1}{32}\cos 3\omega_0 t + \frac{10}{4}\Big) \tag{16}$$

3 Nonlinear Control Design

The control objective is to drive the deflection of the tip of the piezoelectric nanoactuator to a desired oscillation. To this end, Eq. (5) is expressed as:

$$\ddot{\mathbf{q}}(t) = \mathbf{F}(\mathbf{q}(t)) + \boldsymbol{\beta}\mathbf{u}(\tau) + \mathbf{d}(\tau) \tag{17}$$

where $\mathbf{d}(\tau)$ is the vector of bounded external disturbances and

$$\mathbf{F}(\mathbf{q}) = \hat{\boldsymbol{F}}(\mathbf{q}) + \Delta\mathbf{F}(\mathbf{q}) \\ \boldsymbol{\beta} = \hat{\boldsymbol{\beta}} + \Delta\boldsymbol{\beta} \quad \text{and} \quad \mathbf{u}(\tau) = \mathbf{E}V_0(\tau) \tag{18}$$

The $\hat{\boldsymbol{F}}$ and $\hat{\boldsymbol{\beta}}$ are known real constant matrices, and $\Delta()$ are unknown matrices representing system parameter uncertainties therefore:

$$\hat{\boldsymbol{F}}(\mathbf{q}) = -\mathbf{M}^{-1}(\mathbf{K}\mathbf{q} + \boldsymbol{\beta}\mathbf{q}^3) \quad \text{and} \quad \hat{\boldsymbol{\beta}} = \mathbf{M}^{-1}\mathbf{E} \tag{19}$$

For the control design purpose, it is convenient to rewrite the ODE, i.e., Eq. (5), into a state space model.

3.1 State Space Model

For the system defined by Eq. (17), controllability condition is given by $\boldsymbol{\beta} \neq 0$ and the state space representation as:

$$\mathbf{q}(t) = (\mathbf{q}^T, \dot{\mathbf{q}}^T)^T \quad \epsilon R^{2n} \tag{20}$$

$$u(t) = V_0(t) \tag{21}$$

To design a controller, deflection of the tip of the flexoelectric nanoactuator is considered as a control output and is given by:

$$y = \mathbf{H}\mathbf{x} \tag{22}$$

where vector $\mathbf{H}$ is defined as:

$$\mathbf{H} = [\phi_1(1) \quad \phi_2(1) \ldots \phi_n(1) \quad \mathbf{0}_{1\times n}] \tag{23}$$

It is assumed that $\hat{\boldsymbol{\beta}}$ and $\mathbf{M}$ are invertible matrices and well defined and bounded for all time. Also, regarding the system (17), $\hat{\boldsymbol{F}}(\mathbf{q})$ is a continuously differentiable function and the uncertainty terms ($\Delta\mathbf{F}$ and $\Delta\boldsymbol{\beta}$) are assumed to be bounded by:

$$|\Delta\mathbf{F}| = |\mathbf{F} - \hat{\mathbf{F}}| \le \Pi \\ |\Delta\boldsymbol{\beta}| = |\boldsymbol{\beta} - \hat{\boldsymbol{\beta}}| \le \boldsymbol{\Lambda} \tag{24}$$

where $\boldsymbol{\Pi}, \boldsymbol{\Lambda} \ge 0$

3.2 Sliding Mode Controller Design

The first step in designing a sliding mode controller is to determine a sliding surface so that the plant restricted to the sliding surface has a desired system response. In this treatise, the sliding surface is represented by:

$$S(\dot{e}, e) = \dot{e} + \lambda e = 0 \tag{25}$$

where λ is an positive value that must satisfy the Hurwitz condition, and e is tracking error. The tracking error and its derivative value are obtained as:

$$e = \mathbf{H}\mathbf{q} - y_d, \qquad \dot{e} = \mathbf{H}\dot{\mathbf{q}} - \dot{y}_d \tag{26}$$

In Eq. (26), y_d is the desired path (reference input) for tracking.

The next step is designing a switched feedback gains necessary to drive the state trajectory to the sliding surface. These constructions are built on the generalized Lyapunov stability theory. So, the control input for only one mode (first mode) is considered as follows:

$$u(t) = u_{\mathrm{eq}} + u_c \tag{27}$$

where u_{eq} is the equivalent control term and u_c is considered for tracking, despite the uncertainties and disturbances. u_{eq} can be designed based on the Filippov's equivalent dynamics which states that $\dot{S}(\dot{e}, e) = 0$, while the dynamics is on the sliding mode. For the first mode in this case:

$$\dot{S}(\dot{e}, e) = \ddot{e} + \lambda\dot{e} = H\ddot{q} - \ddot{y}_d + \lambda\big(H\dot{q} - \dot{y}_d\big) = 0 \tag{28}$$

Therefore, considering Eqs. (17) and (18), one can obtain:

$$H(\hat{F}(q) + \hat{\beta}u_{\mathrm{eq}}(\tau)) - \ddot{y}_d + \lambda\big(H\dot{q} - \dot{y}_d\big) = 0 \tag{29}$$

By reshuffling Eq. (29), u_{eq} can be expressed as:

$$u_{\mathrm{eq}}(\tau) = \big[H\hat{\beta}\big]^{-1}\Big\{\ddot{y}_d - \lambda\big(H\dot{q} - \dot{y}_d\big) - H\hat{F}(q)\Big\} \tag{30}$$

As previously stated, u_c will be added to the control input in order to prove the stability and robustness of the equivalent control term, i.e., Eq. (30). To ensure the asymptotic stability of the system, the u_c must be determined in a way that the derivative of the system's Lyapunov function is given negative. In order to achieve this goal, u_c is considered as follows:

$$u_c = -\left\{ \left[H\hat{\beta}\right]^{-1} k \right\} \mathrm{Sign}(s) \tag{31}$$

3.3 Stability Analysis

In order to proof the asymptotic stability and the reliability of a given controller, the Lyapunov function is considered as $V = \frac{1}{2}S^2$; therefore, the derivative of Lyapunov function is:

$$\dot{V} = S\dot{S} \le -\Gamma|S|, \quad S \ne 0 \tag{32}$$

In Eq. (32), Γ is a positive arbitrary constant. By inserting Eqs. (30) and (31) in Eq. (27), the control input is obtained:

$$\begin{aligned} u(t) &= u_{\mathrm{eq}} + u_c \\ &= \left[H\hat{\beta}\right]^{-1} \left\{ \ddot{y}_d - \lambda\left(H\dot{q} - \dot{y}_d\right) - H\hat{F}(q) - k\mathrm{Sign}(s) \right\} \end{aligned} \tag{33}$$

Substituting Eq. (33) into Eq. (17) and considering Eq. (18), one can obtain:

$$\begin{aligned} \ddot{q} = \hat{F}(q) + \Delta F(q) + \left(\hat{\beta} + \Delta\beta\right) \\ \left[H\hat{\beta}\right]^{-1} \left\{ \ddot{y}_d - \lambda\left(H\dot{q} - \dot{y}_d\right) - H\hat{F}(q) - k\mathrm{Sign}(s) \right\} \end{aligned} \tag{34}$$

By substituting Eq. (34) into Eq. (28), the derivative of the Lyapunov function is obtained as follows:

$$\begin{aligned} \dot{V} = S\Big[H\Big\{ \hat{F}(q) + \Delta F(q) + (\hat{\beta} + \Delta\beta)[H\hat{\beta}]^{-1} \\ \left\{ \ddot{y}_d - \lambda(H\dot{q} - \dot{y}_d) - H\hat{F}(q) - kSign(s) \right\} \Big\} \\ - \ddot{y}_d + \lambda(H\dot{q} - \dot{y}_d)\Big] \end{aligned} \tag{35}$$

Considering Eq. (29) and simplifying Eq. (35) result in:

$$\dot{V} = S\left(H\Delta F(q) + \hat{\beta}^{-1}\Delta\beta\psi\right) - \eta k|S| \tag{36}$$

where

$$\psi = \ddot{y}_d - \lambda\left(H\dot{q} - \dot{y}_d\right) - H\hat{F}(q)\eta = 1 + \hat{\beta}^{-1}\Delta\beta \tag{37}$$

Now, if the condition $\dot{V} = S\dot{S} \le -\Gamma|S|$ is established, the asymptomatic stability of the system is guaranteed, to do this:

$$S\left(H\Delta F(q) + \hat{\beta}^{-1}\Delta\beta\psi\right) - \eta k|S| \le -\Gamma|S| \tag{38}$$

In this case, if $S = 0$, the condition (38) is satisfied, and if S is positive, it is concluded that in worst case:

$$\left(H\Delta F(q) + \hat{\beta}^{-1}\Delta\beta\psi\right) - \eta k \le -\Gamma \tag{39}$$

Therefore, if

$$k \ge \frac{1}{\eta}\left\{ \Gamma + \left(H\Delta F(q) + \hat{\beta}^{-1}\Delta\beta\psi\right) \right\}, \tag{40}$$

stability conditions are satisfied, and if S is negative, the stability conditions will be as follows:

$$k \ge \frac{1}{\eta}\left\{ \Gamma - \left(H\Delta F(q) + \hat{\beta}^{-1}\Delta\beta\psi\right) \right\} \tag{41}$$

4 Numerical Results and Discussion

As it is known, flexoelectricity effect plays a significant role just at micro-/nanoscales. Hence, for more illustration, in this paper, a cantilever flexoelectric nanobeam (CPNB) is considered for analysis which is made of $BaTiO_3$. The corresponding geometrical and material data are listed in Table 1. Henceforth, all the employed parameters are same as in Table 1 unless new data are prescribed.

To verify the current results, the obtained Galerkin outcomes for the static deflection due to a constant applied voltage are compared with the available linear analytical results which is accessible in Tadi Beni (2016a) and the current *bvp4c* results. The comparison is depicted in Fig. 2 for $V_0 = 4000v$ by the consideration of one and three linear normal modes in Galerkin projection. A very good agreement is clear between the current three-mode Galerkin projection, the *bvp4c* method and the analytical results. Because the Galerkin approach is very handy in the implementation hence, hereafter, three-mode Galerkin technique is employed for the static deflection computations.

Table 1 The geometrical and material data of the assumed piezoelectric nanobeam (Tadi Beni 2016a)

Parameter	Description	Value (unit)
L	Beam length	500 (nm)
b	Beam width	10 (nm)
h	Beam thickness	15 (nm)
l	Scale factor	0.2 h
f	Flexoelectric coefficient	$5e^{-12}$ (C/m)
μ	Lame constant	42.9 (GPa)
λ	Lame constant	45.2 (GPa)

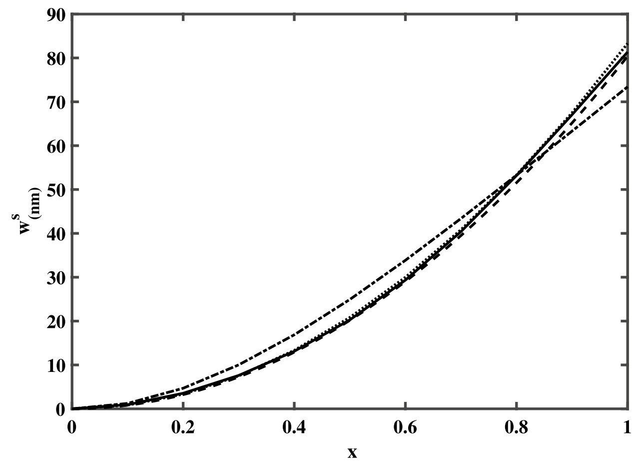

Fig. 2 The current nonlinear static deflection achieved by one-mode Galerkin technique (dotted-dashed lines), three-mode Galerkin technique (solid lines) and the *bvp*4*c*-subroutine (dashed lines) versus the corresponding linear analytical results of Tadi Beni (2016b) (dotted lines): ($V_0 = 4000v$)

Table 2 The current first two linear natural frequencies in comparison with those of Arvin (2018) (MHz)

Frequency	Results of Arvin (2018)	Current results	Error
ω_1	0.3108	0.3107	0.03
ω_2	1.9326	1.9468	0.73

Another verification is confirmed in calculation of linear natural frequency in comparison with Arvin (2018). The considered beam is a rotating nanocantilever beam which is made of epoxy with the mass density, Young's modulus, the Poisson ratio and the material length scale parameter, respectively, equal to $\rho = 1220\ \text{kg/m}^3$, $E = 1.4$ GPa, $\nu = 0.3$ and $l = 17.6\ \mu\text{m}$. The slenderness ratio, i.e., $S = L\sqrt{\frac{A}{I}}$, and height to material scale parameter, i.e., $\upsilon = \frac{h}{l}$, are given, respectively, as $S = 30$ and $\upsilon = 1$. In slenderness ratio, L, A and I are, respectively, the beam length, the beam cross-sectional area and the beam moment of inertia about y-axis (see Fig. 1). As the considered nanobeam is a rotating beam, the dimensionless rotation speed is considered as $\lambda_R = 0$ in Fig. 9 of Arvin (2018). The compared results for the first two linear natural frequencies are shown in Table 2. The results show a very good agreement. It should be noted that in Arvin (2018), the rotary inertia influences are taken into account, and hence, the neglecting of rotary inertia here seems reasonable.

After confirming the current results, some case studies are addressed here.

4.1 Case Studies: Nonlinear Vibration

The effects of the length scale parameter and the flexoelectric constant on the nonlinear natural frequency of the given CFNB are examined here.

The effects of length scale parameter to beam thickness ratio, i.e., l/h, on the nonlinear natural frequency in terms of beam tip displacement and the applied voltage are presented, respectively, in Fig. 3a, b. The x-axis defines the ratio of the nonlinear natural frequency with respect to the corresponding linear natural frequency for $l/h = 0$. A hardening behavior for the first mode is obvious. For verification of the predicted treatment, it can be mention that when just the geometric nonlinearities are considered, for the cantilever beam imposing the inextensibility condition,

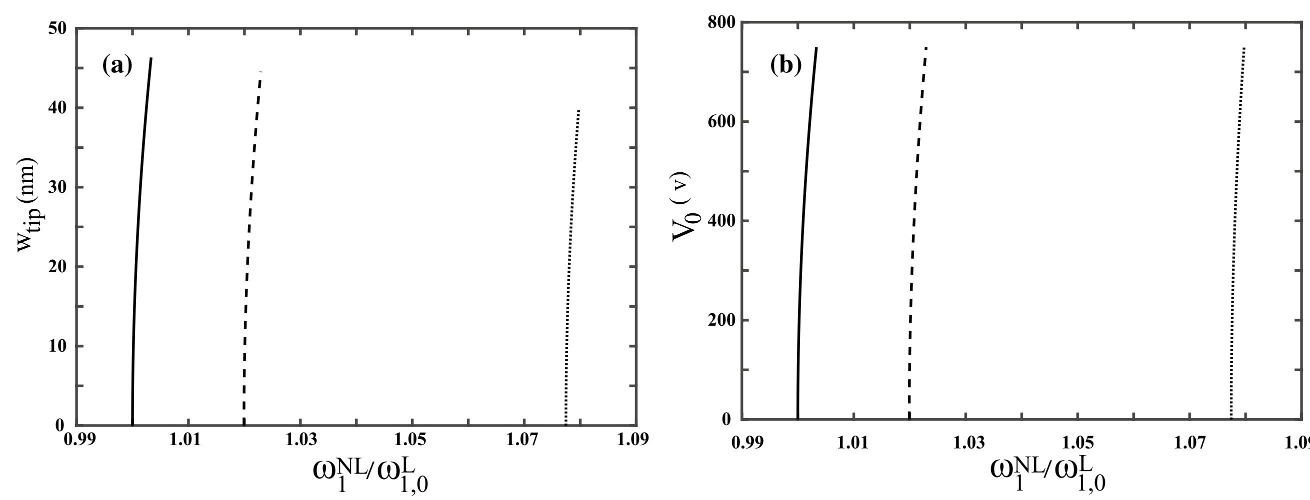

Fig. 3 The effect of the length scale parameter to beam thickness ratio, i.e., *l*/*h*, on the nonlinear natural frequency in terms of: **a** beam tip displacement and **b** the applied voltage (solid lines, $l/h = 0$, dashed lines, $l/h = 0.05$, and dotted lines, $l/h = 0.1$)

the hardening behavior is expected (see McHugh and Dowell 2018). It can be seen that by increasing l/h parameter due to the stiffening of the beam structure, the linear and subsequently the nonlinear natural frequencies increase. On the other hand, more stiffen structure is exposed to the lower deflection at the same applied voltage.

The effects of the flexoelectric constant on the first nonlinear natural frequency in terms of the applied voltage are presented in Fig. 4. It can be inferred that as it is expected, the flexoelectric constant does not change the linear natural frequency because it does not have any contributions in the linear structural stiffness. On the contrast, because the increment in its magnitude enhances the beam deflection, it makes the nonlinear structural stiffness stiffer, and hence, the nonlinear natural frequency increases.

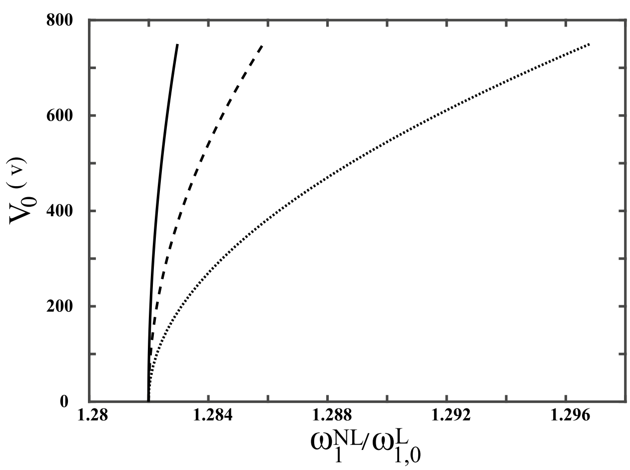

Fig. 4 The effect of flexoelectric constant on the first nonlinear natural frequency in terms of applied voltage (solid lines, $f = 5\,\mathrm{pC/m}$, dashed lines, $f = 10\,\mathrm{pC/m}$, and dotted lines, $f = 20\,\mathrm{pC/m}$)

4.2 Case Studies: Nonlinear Control

Nonlinear control simulation of the tip of the nanoflexoelectric cantilever actuator is carried out by employing sliding mode. To reduce the chattering effect, the saturation function is used in sliding mode control.

In order to examine the performance of the nonlinear controller, the designed sliding mode controller is compared with the linear fuzzy controller which is accessible in Ref. Vaghefpour et al. (2018). Figures 5 and 6 illustrate nonlinear and fuzzy linear tip tracking for the sinusoidal input, respectively. In order to verify the robustness of the sliding mode controller, a disturbance pulse signal is applied in the fifth second of the simulation. Figure 5 shows that the sliding mode controller can successfully track the reference signal (R) with a very small error, and by applying the disturbance (pulse) in 5 s of simulation, tracking is carried out with a very low oscillation range (1%) and a low settling time (about 1 s).

In Fig. 6, the fuzzy controller tracking for the sinusoidal input is shown (Vaghefpour et al. (2018)). By comparing Figs. 5 and 6, it can be seen that the tracking in the nonlinear controller is more favorable than the fuzzy controller, while the fuzzy controller is more resistant than the nonlinear controller.

The tracking errors of nonlinear sliding mode and linear fuzzy controllers are illustrated in Figs. 7 and 8. It can be inferred that the both controllers are good robust controller, whereas the fuzzy controller is more robust than sliding mode controller.

Figures 7 and 8 indicate that the error in the sliding mode controller is very low and close to zero in the absence of external disturbance, while in the fuzzy controller, the trajectory of the path is smooth with an approximate error of 20%. By applying external disturbance, the error in the sliding mode controller increases to 100%; however, the external disturbance has a very small effect on the performance of the fuzzy controller.

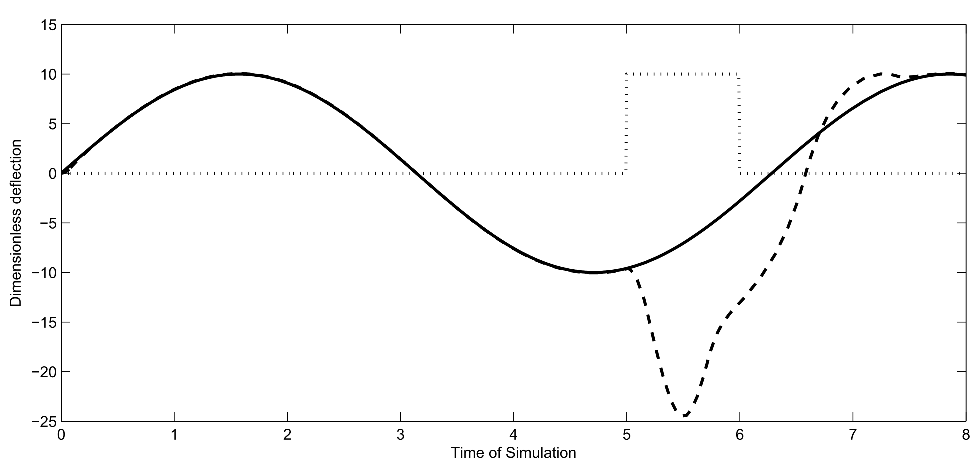

Fig. 5 Nonlinear tip tracking control (dashed lines) with sinusoidal wave reference input (solid lines) and a pulse disturbance (dotted lines) at time of simulation 5

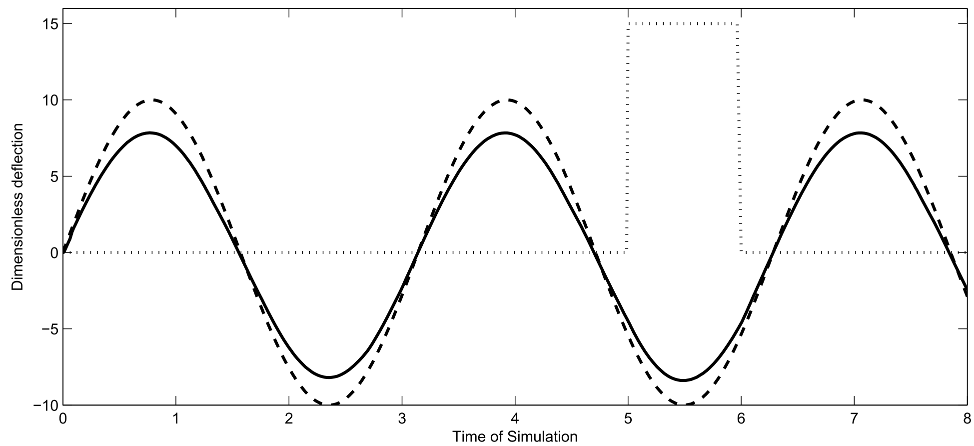

Fig. 6 Linear fuzzy control (dashed lines) with sinusoidal wave reference input (solid lines) and a pulse disturbance (dotted lines) at time of simulation 5

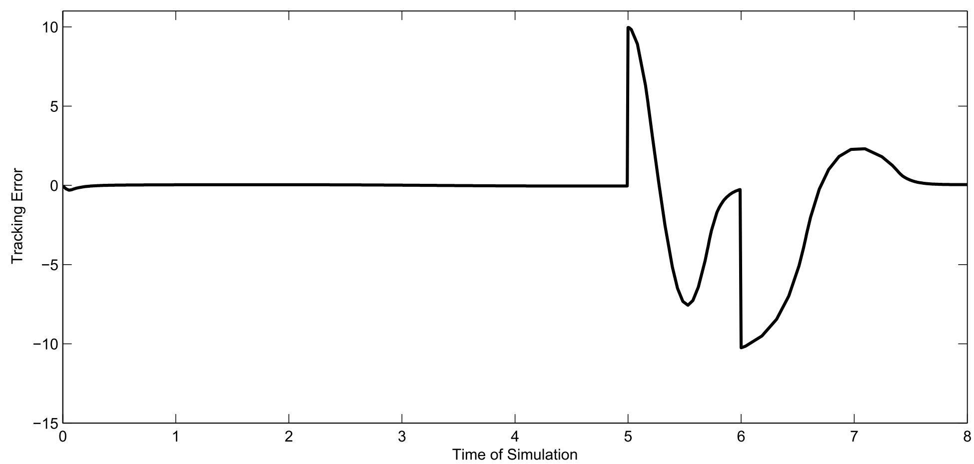

Fig. 7 Nonlinear tracking error with sinusoidal wave reference input and a pulse disturbance at time of simulation 5

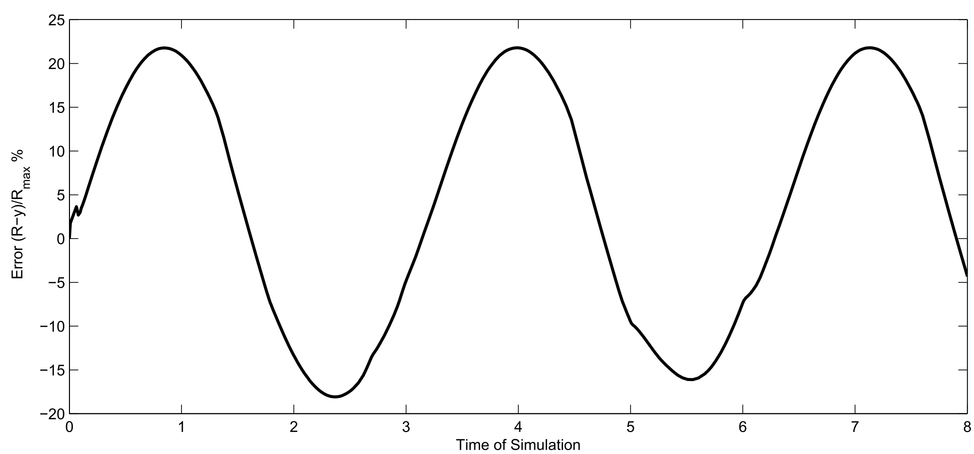

Fig. 8 Linear fuzzy error with sinusoidal wave reference input and a pulse disturbance at time of simulation 5

Figures 9 and 10 show applied voltage as the input control.

As shown in Figs. 9 and 10, the input voltage for tracking the sinusoidal path in the fuzzy controller is more than sliding mode controller.

5 Summary and Conclusion

The nonlinear modeling and tip tracking control of an inextensible flexoelectric cantilever nanoactuator were

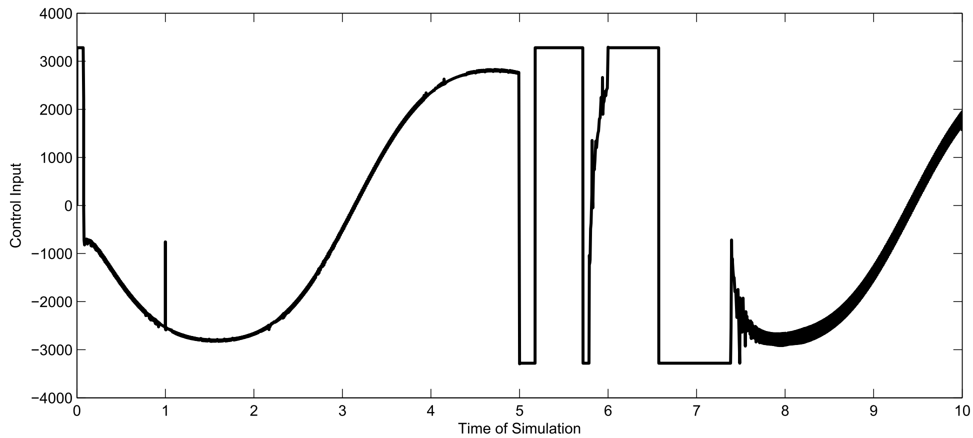

Fig. 9 Nonlinear tracking input control with sinusoidal wave reference input and a pulse disturbance at time of simulation 5

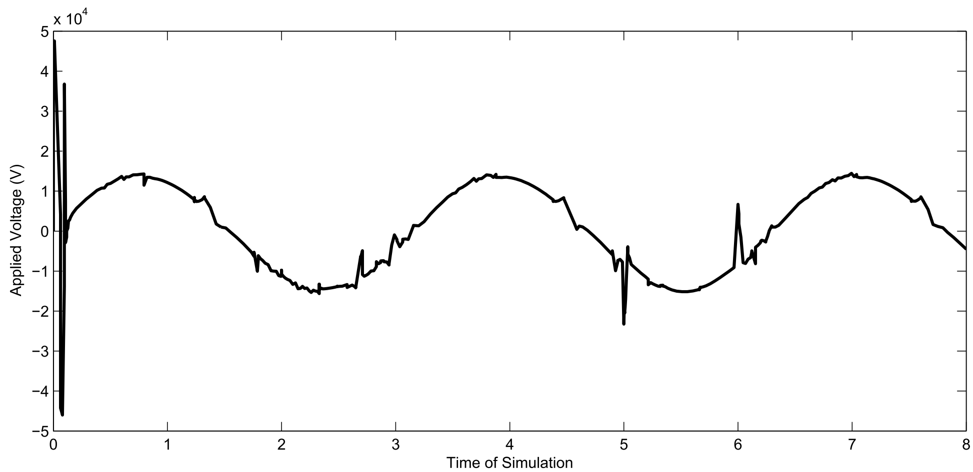

Fig. 10 Linear fuzzy input control with sinusoidal wave reference input and a pulse disturbance at time of simulation 5

investigated based on the size-dependent piezoelectric theory besides a higher-order curvature relation. The results of vibration analysis and performance of nonlinear sliding mode controller of cantilever flexoelectric nanoactuators were presented. The perturbation method was implemented to solve the nonlinear ODE for the nonlinear vibration examination. The influences of the applied voltage, the material length scale parameter with respect to the beam thickness ratio and the flexoelectric coefficient on the nonlinear natural frequency of the assumed cantilever flexoelectric nanoactuator were discussed. At the end, the results of nonlinear sliding mode controller for nanoactuator were studied. In order to compare the performance of the linear fuzzy controller and nonlinear controller, some figures were considered. Referring to the numerical results, it can be deduced that:

(1) Due to hardening effect of scale factor on the linear stiffness of the nanobeam, by increasing the scale factor to the beam thickness ratio, the existing discrepancy between the linear and the nonlinear static deflections reduces; (2) by increasing the flexoelectric coefficient and/or the applied voltage, the difference between the linear and the nonlinear static deflection increases; (3) the increment in the scale factor to the beam thickness ratio increases the linear and nonlinear natural frequency; (4) the flexoelectric does not have any contribution in the linear natural frequency, while the increment in its magnitude increases the nonlinear natural frequency; (5) the input voltage in the nonlinear controller is much less than the linear controller; (6) the fuzzy controller is more robust than sliding mode controller; (7) the comparison results show that nonlinear control performance of the proposed sliding mode is better than that of linear methods used to resolve the same problem (Vaghefpour et al. 2018) in terms of the steady-state error.

References

Akgoz B, Civalek O (2012) Longitudinal vibration analysis for microbars based on strain gradient elasticity theory. J Vib Control 20:1–11

Akgoz B, Civalek O (2013) Free vibration analysis of axially functionally graded tapered Bernoulli-Euler microbeams based on the modified couple stress theory. Compos Struct 98:314–322

Akgoz B, Civalek O (2017) Effects of thermal and shear deformation on vibration response of functionally graded thick composite microbeams. Compos Part B. https://doi.org/10.1016/j.compositesb.2017.07.024

Alsaleem FM, Younis MI (2011) Integrity analysis of electrically actuated resonators with delayed feedback controller. J Dyn Syst Meas Control Trans ASME 133(3):031011-1–051003-8

Ansari R, Mohammadi V, Faghih Shojaei M, Gholami R, Sahmani S (2013) Post buckling characteristics of nanobeams based on the surface elasticity theory. Compos Part B Eng 55:240–246

Arani AG, Abdollahian M, Kolahchi R (2015) Nonlinear vibration of a nanobeam elastically bonded with a piezoelectric nanobeam via strain gradient theory. Int J Mech Sci 100:32–40

Arefia M, Pourjamshidian M, Ghorbanpour AA (2018) Free vibration analysis of a piezoelectric curved sandwich nano-beam with FG-CNTRCs face-sheets based on various high-order shear deformation and nonlocal elasticity theories. Eur Phys J Plus 133:193

Arvin H (2018) The flapwise bending free vibration analysis of micro-rotating Timoshenko beams using the differential transform method. J Vib Control 24(20):4868–4884. https://doi.org/10.1177/1077546317736706

Barari A, Kaliji HD, Ghadimi M, Domairry G (2011) Non-linear vibration of Euler–Bernoulli beams. Lat Am J Solids Struct 8:139–148

Baskaran S, He X, Chen Q, Fu JF (2011) Experimental studies on the direct flexoelectric effect in a phase polyvinylidene fluoride films. Appl Phys Lett 98:242901

Cao J, Syta A, Litak G, Zhou S, Inman DJ, Chen Y (2015) Regular and chaotic vibration in a piezoelectric energy harvester with fractional damping. Eur Phys J Plus 130:103

Casadei F, Dozio L, Ruzzene M, Cunefare KA (2010) Periodic shunted arrays for the control of noise radiation in an enclosure. J Sound Vib 329:3632–3646

Cross LE (2006) Flexoelectric effects: charge separation in insulating solids subjected to elastic strain gradients. J Mater Sci 41:53–63

Donthireddy P, Chandrashekhara K (1996) Modeling and shape control of composite beams with embedded piezoelectric actuators. Compos Struct 35:237–244

Ebnali Samani MS, Tadi Beni Y (2018) Size dependent thermo-mechanical buckling of the flexoelectric nanobeam. Mater Res Express 5(8):085018

Ebrahimia F, Barati MR (2017a) Magnetic field effects on buckling characteristics of smart flexoelectrically actuated piezoelectric nanobeams based on nonlocal and surface elasticity theories. Microsyst Technol. https://doi.org/10.1007/s00542-017-3652-x

Ebrahimi F, Barati MR (2017b) Free vibration analysis of couple stress rotating nanobeams with surface effect under in-plane axial magnetic field. Eur Phys J Plus 132:19

Ebrahimi F, Dehghan M, Seyfi A (2019) Eringen's nonlocal elasticity theory for wave propagation analysis of magneto-electro-elastic nanotubes. Adv Nano Res 7(1):1–11

Esmaeili M, Beni YT (2019) Vibration and buckling analysis of functionally graded flexoelectric smart beam. J Appl Comput Mec. 5(5):900–917

Hadjesfandiari AR (2013) Size-dependent piezoelectricity. Int J Solids Struct 50:2781–2791

Hadjesfandiari AR, Dargush FG (2011) Couple stress theory for solids. Int J Solids Struct 48:2496–2510

Hao Z, Liao B (2010) An analytical study on interfacial dissipation in piezoelectric rectangular block resonators with in-plane longitudinal- mode vibrations. Sens Actuators A Phys 163:401–409

Ke LL, Wang YS, Wang ZD (2012) Nonlinear vibration of the piezoelectric nanobeams based on the nonlocal theory. Compos Struct 94:2038–2047

Koszewnika A (2018) The design of a vibration control system for an aluminum plate with piezo-stripes based on residues analysis of model. Eur Phys J Plus 133:405

Krysko VA Jr, Awrejcewicz J, Dobriyan V, Papkova IV, Krysko VA (2019) Size-dependent parameter cancels chaotic vibrations of flexible shallow nano-shells. J Sound Vib. https://doi.org/10.1016/j.jsv.2019.01.032

Liu YF, Li J, Hu XH, Zhang ZM, Cheng L, Lin Y, Zhang WA (2015) Piezoelectric array for sensing vibration modal coordinates. J Mech Sci 6:95–107

Managheb SAM, Ziaei-Rad S, Tikani R (2018) Energy harvesting from vibration of Timoshenko nanobeam under base excitation considering flexoelectric and elastic strain gradient effects. J Sound Vib 421:166e189

Maranganti R, Sharma ND, Sharma P (2006) Electromechanical coupling in nonpiezoelectric materials due to nanoscale nonlocal size effects: Green's function solutions and embedded inclusions. Phys Rev B 74:14110-1–14110-14

McHugh K, Dowell E (2018) Nonlinear responses of inextensible cantilever and free-free beams undergoing large deflections. J Appl Mech 85:051008-1-8

Mishima T, Fujioka H, Nagakari S, Kamigake K, Nambu S (1997) Lattice image observations of nanoscale ordered regions in Pb (Mg1/3Nb2/3)O-3. Jpn J Appl Phys 36:6141–6144

Nateghi A, Salamat-talab M, Rezapoure J, Daneshian B, (2012) Size dependent buckling analysis of functionally graded Timoshenko micro beams based on modified couple stress theory. In: Mechanics of Nano, Micro and Macro Composite Structures, pp 18–20

Numanoglu HM, Akgöz B, Civalek ö (2018) On dynamic analysis of nanorods. Int J Eng Sci 130:33–50

Quoc CN, Slava K (2015) Nonlinear tracking control of vibration amplitude for a parametrically excited microcantilever beam. J Sound Vib 338:91–104

Rafiepour H, Lotfavar A, Masroori A (2013) Analytical approximate solution for nonlinear vibration of microelectromechanical system using he's frequency amplitude formulation. Iran J Sci Technol Trans Mech Eng 37:83–90

Rojas EF, Faroughi S, Abdelkefi A, Park YH (2019) Nonlinear size dependent modeling and performance analysis of flexoelectric energy harvesters. Microsyst Technol. https://doi.org/10.1007/s00542-019-04348-9

Seleim A, Towfighian S, Delande E, Abdel-Rahman E, Heppler G (2012) Dynamics of a close-loop controlled MEMS resonator. Nonlinear Dyn 69:615–633

Shao S, Masri KM, Younis MI (2013) The effect of time-delayed feedback controller on an electrically actuated resonator. Nonlinear Dyn 74:257–270

Siewe MS, Hegazy UH (2011) Homoclinic bifurcation and chaos control in MEMS resonators. Appl Math Model 35:5533–5552

Sumali H, Meissner K, Cudney HH (2001) A piezoelectric array for sensing vibration modal coordinates. Sens Actuators A Phys 93:123–131

Tadi Beni Y (2016a) A nonlinear electro-mechanical analysis of nanobeams based on the size-dependent piezoelectricity theory. J Mech 1–13

Tadi Beni Y (2016b) Size-dependent electromechanical bending, buckling and free vibration analysis of functionally graded piezoelectric nanobeams. J Intell Mater Syst Struct. https://doi.org/10.1177/1045389X15624798

Vaghefpour H, Arvin H (2019) Nonlinear free vibration analysis of pre-actuated isotropic piezoelectric cantilever Nano-beams. Microsyst Technol. https://doi.org/10.1007/s00542-019-0

Vaghefpour H, Arvin H, Tadi Y (2018) Tip tracking control of piezoelectric nano-actuator with flexoelectric size-dependent theory. AmirKabir J Sci Res. https://doi.org/10.22060/MEJ.2018.14089.5795

Vatankhah R, Najafi A, Salarieh H, Alasty A (2013) Boundary stabilization of non-classical micro-scale beams. Appl Math Model. 37:8709–8724

Wang PKC (1998) Feedback control of vibrations in mircomachined cantileverbeam with electrostatic actuators. J Sound Vib 213(3):537–550

Yekrangisendi A, Yaghobi M, Riazian M, Koochi A (2019) Scale-dependent dynamic behavior of nanowire-based sensor in accelerating field. J Appl Comput Mech 5(2):486–497